

MIT Open Access Articles

On the roles of smoothing in planning of informative paths

The MIT Faculty has made this article openly available. **Please share** how this access benefits you. Your story matters.

Citation: Han-Lim Choi, and J.P. How. "On the roles of smoothing in planning of informative paths." American Control Conference, 2009. ACC '09. 2009. 2154-2159. © Copyright 2009 IEEE

As Published: <http://dx.doi.org/10.1109/ACC.2009.5160721>

Publisher: Institute of Electrical and Electronics Engineers

Persistent URL: <http://hdl.handle.net/1721.1/58892>

Version: Final published version: final published article, as it appeared in a journal, conference proceedings, or other formally published context

Terms of Use: Article is made available in accordance with the publisher's policy and may be subject to US copyright law. Please refer to the publisher's site for terms of use.



On the Roles of Smoothing in Planning of Informative Paths

Han-Lim Choi and Jonathan P. How

Abstract—This paper investigates the roles of smoothing in planning of information-gathering paths for mobile sensors, when the goal is to minimize the entropy of some variables of interest at the final time of generated plan. The main result is that smoothing simplifies the process of calculating the information gathered up to some arbitrary time on the fly. This enables quantification of the *correct* cost-to-go value when applied to a receding-horizon approximation of the optimal path planning problem. Numerical examples on simplified weather forecasting, sensor scheduling, and target localization validate the theoretical findings.

I. INTRODUCTION

One key problem for (mobile) sensor networks is to create plans for maneuvering/locating the sensing resources in order to extract information from the environment. A typical goal is to reduce uncertainty in some quantities of interest, called the verification variables (e.g., position and velocity of targets [1]–[8], the pose of the sensor platform itself, the forecast of weather over some region of interest [9]–[13], or physical quantities under the ocean [14]) by designing measurement paths for (mobile) sensors over some time window $[0, \tau]$. Mutual information is often used as an information-theoretic metric for the uncertainty reduction. The mutual information between the verification variables and some measurement sequence over $[0, \tau]$ represents the difference between the prior and the posterior entropy of the verification variables when conditioned on this sequence of measurements. Thus, it explicitly quantifies the impact of sensing on the entropy reduction of the quantity of interest.

Depending on the time when one is interested in the value of the verification variables, two types of planning problems can be posed: the *tracking* problem and the *forecasting* problem. The objective of the tracking problem is to minimize the uncertainty in the verification variables at time τ , i.e. at the end of the planning window, whereas the forecasting problem is concerned with the uncertainty in the verification variables at some time T in the far future ($T \gg \tau$). While most previous work [1]–[4,6,8] on information-theoretic planning had addressed the tracking problem, the present authors have proposed information-theoretic methodologies for the forecasting problem [10]–[13]. In particular, it was demonstrated in [12,13] that the well-known conditional independence of past variables and future variables given the present state provides key insights to efficiently and correctly quantify the mutual information for the forecasting problem. The smoothing approach, proposed in these works enables the calculation of the mutual

information between the verification variables at T and a measurement path over $[0, \tau]$ as the difference between the unconditioned and conditioned mutual information between the state at τ and the respective measurement path. The results in [12,13] reduce the length of the time interval over which the matrix differential equations must be integrated, provide on-the-fly access to the accumulated information, and correctly quantify the information-gathering rate.

This paper expands these roles of smoothing identified for the forecasting problem to the tracking problem. In particular, it will be shown that the smoothing approach enables correct quantification of cost-to-go values in a receding-horizon approximation of the tracking problem. New insights on the influence of the choice of the verification variables and the presence of process noise on the mutual information is discussed. Extensive numerical studies with three representative informative planning problems are performed to illustrate and verify the suggested roles of smoothing in the tracking problems.

II. PROBLEM DEFINITION

A. Linear System Model

Consider the dynamics of objects/environment with finite dimensional state vector $X_t \in \mathbb{R}^n$ described by the following linear time-varying system:

$$\dot{X}_t = A(t)X_t + W_t \quad (1)$$

where $W_t \in \mathbb{R}^n$ is a zero-mean Gaussian process noise with $\mathbb{E}[W_t W_s'] = \Sigma_W \delta(t - s)$, $\Sigma_W \succeq 0$, which is independent of X_t . The prime sign ($'$) denotes the transpose of a matrix. The initial condition of the state, X_0 is normally distributed as $X_0 \sim \mathcal{N}(\mu_0, P_0)$, $P_0 \succ 0$.

The system (1) is observed by sensors with additive Gaussian noise and admits the following measurement model for $Z_t \in \mathbb{R}^m$:

$$Z_t = C(t)X_t + N_t \quad (2)$$

where $N_t \in \mathbb{R}^m$ is zero-mean Gaussian with $\mathbb{E}[N_t N_s'] = \Sigma_N \delta(t - s)$, $\Sigma_N \succ 0$, which is independent of X_t and W_s , $\forall s$. Also, a measurement history over the time window $[t_1, t_2]$ is defined as

$$\mathcal{Z}_{[t_1, t_2]} = \{Z_t : t \in [t_1, t_2]\}. \quad (3)$$

The verification variables are a subset of the state variables that are of interest to define the performance measure, and are defined as

$$V_t = M_V X_t \in \mathbb{R}^p \quad (4)$$

where $M_V \in \{0, 1\}^{p \times n}$, $p < n$ with every row-sum of M_V being unity. Although this work is specifically focused the

H. -L. Choi and J. P. How are with the Dept. of Aeronautics and Astronautics, MIT, Cambridge, MA 02139, USA, {hanlimc, jhow}@mit.edu

case where entries of M_V are zero or one, the results can be easily extended to a general $M_V \in \mathbb{R}^{p \times n}$.

B. Optimal Tracking Problem

Using entropy as the metric of uncertainty, the uncertainty reduction of the verification variables by measurements taken along the path of the sensors can be represented by the mutual information. Then, the optimal tracking problem can be written as the following optimization problem:

$$\max_{\mathcal{Z}_{[0,\tau]}} \mathcal{I}(V_\tau; \mathcal{Z}_{[0,\tau]}) \quad (\text{OTP})$$

where $\mathcal{I}(Y_1; Y_2)$ represents the mutual information between two random quantities Y_1 and Y_2 (e.g. random variables, random processes, random functions). In other words, (OTP) finds the best (continuous) measurement history over $[0, \tau]$ that achieves the largest entropy reduction of the verification variables at τ .

In (OTP), it is assumed that the measurement at a given time t is dependent on the location of the sensors at that time: i.e. $Z_t = Z_t(\mathbf{r}(t))$ where $\mathbf{r}(t)$ denotes the locations of sensors at t . Given the measurement model in (2), this represents the cases where either the observation matrix $C(t)$ and/or the measurement noise variance Σ_N is a function of sensor locations. This work specifically considers the first case without loss of generality. Since the motion of sensor platforms are constrained, the resulting path planning problem is to maximize the objective function in (OTP) subject to various types of constraints induced by vehicle motion and the specific applications. Receding-horizon approximations of (OTP) will be discussed with further emphasis in section IV.

III. QUANTIFICATION OF MUTUAL INFORMATION

For the linear system, the objective value for (OTP) can be computed as

$$\mathcal{I}(V_\tau; \mathcal{Z}_{[0,\tau]}) = \frac{1}{2} \text{ldet } P_V(\tau) - \frac{1}{2} \text{ldet } Q_V(\tau) \quad (5)$$

where ldet stands for $\log \det$, $P_V(\tau) \triangleq \text{Cov}[V_\tau]$ and $Q_V(\tau) \triangleq \text{Cov}[V_\tau | \mathcal{Z}_{[0,\tau]}]$; these two matrices can be written as $P_V = M_V P_X M_V'$, and $Q_V = M_V Q_X M_V'$ where P_X and Q_X are obtained by integrating (forward in time) the following matrix differential equations:

$$\dot{P}_X(t) = A(t)P_X(t) + P_X(t)A'(t) + \Sigma_W \quad (6)$$

$$\begin{aligned} \dot{Q}_X(t) &= A(t)Q_X(t) + Q_X(t)A'(t) \\ &\quad + \Sigma_W - Q_X(t)C(t)'\Sigma_N^{-1}C(t)Q_X(t) \end{aligned} \quad (7)$$

with initial condition, $P_X(0) = Q_X(0) = P_0$. Notice that (6) is Lyapunov equation and (7) is the Riccati equation for Kalman-Bucy filters.

Since $P_X(\tau)$ does not depend on the measurement, (OTP) is equivalent to minimizing the posterior entropy $\text{ldet}(M_V Q_X(\tau) M_V')$. Specifically, when $M_V = I$, this becomes equivalent to maximizing the ldet of the Fisher information matrix at time τ , which was addressed in [1].

A. On-the-fly Information

In the process of computing the tracking mutual information $\mathcal{I}(X_\tau; \mathcal{Z}_{[0,\tau]})$ by integrating forward the Lyapunov and Riccati equations in (6) and (7), the only two available matrix quantities are $P_X(t)$ and $Q_X(t)$. Using these, the mutual information between the current state and the measurement thus far, $\mathcal{I}(X_t; \mathcal{Z}_{[0,t]})$ (and that between the current verification variables and the measurement thus far, $\mathcal{I}(V_t; \mathcal{Z}_{[0,t]})$) can be calculated on the fly:

$$\mathcal{I}(X_t; \mathcal{Z}_{[0,t]}) = \frac{1}{2} \text{ldet } P_X(t) - \frac{1}{2} \text{ldet } Q_X(t) \quad (\text{FOI})$$

where the terminology FOI stands for the filter-form on-the-fly information. However, this does not represent the information gathered by $\mathcal{Z}_{[0,t]}$ for the final verification variables V_τ , which is $\mathcal{I}(V_\tau; \mathcal{Z}_{[0,\tau]})$.

This accumulated information for V_τ can be quantified by exploiting the smoothing approach proposed in [12,13]. Since V_τ and $\mathcal{Z}_{[0,t]}$ are conditionally independent of each other for a given X_t , the following expression for the smoother-form on-the-fly information (SOI) can be obtained:

$$\begin{aligned} \mathcal{I}(V_\tau; \mathcal{Z}_{[0,t]}) &= \mathcal{I}(X_t; \mathcal{Z}_{[0,t]}) - \mathcal{I}(X_t; \mathcal{Z}_{[0,t]} | V_\tau) \quad (\text{SOI}) \\ &= \frac{1}{2} [\text{ldet } S_{X|V_\tau}(t) - \text{ldet } S_X(t)] \\ &\quad - \frac{1}{2} \text{ldet} (I + Q_X(t)(S_{X|V_\tau}(t) - S_X(t))) \end{aligned} \quad (8)$$

where $S_{X|V_\tau}(t) \triangleq \text{Cov}(X_t | V_\tau)^{-1}$, which is computed by integrating forward the following differential equation

$$\begin{aligned} \dot{S}_{X|V_\tau} &= -S_{X|V_\tau}(A + \Sigma_W S_X) - (A + \Sigma_W S_X)' S_{X|V_\tau} \\ &\quad + S_{X|V_\tau} \Sigma_W S_{X|V_\tau}. \end{aligned} \quad (9)$$

The initial condition is given by $S_{X|V_\tau}(0) = P_0^{-1}$, which can be expressed as

$$P_0|_{V_\tau} = P_0 - P_0 \Phi_{(\tau,0)}' M_V' P_V(\tau)^{-1} M_V \Phi_{(\tau,0)} P_0$$

where $\Phi_{(\tau,0)}$ is the state transition matrix from time 0 to τ . At $t = \tau$ where the expression in (8) is not well-defined due to singularity of $S_{X|V_\tau}(\tau)$, the value of SOI can be simply computed by (5).

Moreover, the rate of (8) can be expressed as

$$\frac{d}{dt} \mathcal{I}(V_\tau; \mathcal{Z}_{[0,t]}) = \frac{1}{2} \text{tr} \{ \Sigma_N^{-1} C \Pi_\tau(t) C' \}. \quad (10)$$

where $\Pi_\tau \triangleq Q_X(S_{X|V_\tau} - S_X)[I + Q_X(S_{X|V_\tau} - S_X)]^{-1} Q_X$. Notice that the quantity in (10) is non-negative (except at $t = \tau$ where it is not defined), because the effect of the future process noise over $(t, \tau]$ is all encapsulated in $S_{X|V_\tau}$.

To summarize, the smoothing approach allows the true information accumulation and its rate, i.e., $\mathcal{I}(V_\tau; \mathcal{Z}_{[0,t]})$ and $\frac{d}{dt} \mathcal{I}(V_\tau; \mathcal{Z}_{[0,t]})$, to be available for all $t < \tau$ on the fly, by utilizing an additional backward information $S_{X|V_\tau}$ that captures the influence of the future process noise.

IV. INFORMATION FOR RECEDING-HORIZON FORMULATIONS

Despite being theoretically important features, the on-the-fly information quantities may not need to be used if the goal is simply to solve the optimal path planning problems

in (OTP). However, receding-horizon approximations of the original optimization problem are often used due to superior computational efficiency and/or superior adaptability to environmental changes. In this case the computation of on-the-fly information plays a key role, because the effect of a partial measurement history needs to be quantified for a short-horizon subproblem. This section discusses how the on-the-fly information in (8) can be used to determine the cost-to-go functions of the receding-horizon formulations.

Consider a tracking decision for the horizon of $[0, \sigma]$, $\sigma < \tau$ when the ultimate goal is to maximize $\mathcal{I}(V_\tau; \mathcal{Z}_{[0, \tau]})$. For this problem, this work suggests the following formulation based on the smoother-form on-the-fly information:

$$\max_{\mathcal{Z}_{[0, \sigma]}} \mathcal{I}(V_\tau; \mathcal{Z}_{[0, \sigma]}) \equiv \mathcal{I}(X_\sigma; \mathcal{Z}_{[0, \sigma]}) - \mathcal{I}(X_\sigma; \mathcal{Z}_{[0, \sigma]} | V_\tau). \quad (\text{S-RH})$$

In other words, the decision for the time window $[0, \sigma]$ maximizes the smoother-form on-the-fly information at the end of the current planning horizon. Since the time derivative of (SOI) is non-negative over $[0, \tau]$, the objective value of (S-RH) increases as σ increases. It is insightful to contrast (S-RH) to the following formulation based on the filter-form on-the-fly information:

$$\max_{\mathcal{Z}_{[0, \sigma]}} \mathcal{I}(X_\sigma; \mathcal{Z}_{[0, \sigma]}). \quad (\text{F-RH})$$

In other words, (F-RH) aims to minimize the entropy of the current state X_σ , and the underlying premise of this formulation is that an accurate estimate of the current states tends to result in an accurate estimate of the future verification variables.

The formulation (F-RH) is equivalent to the formulation in [1] that maximizes $\text{ldet} Q_X^{-1}(\sigma)$ for the interval $[0, \sigma]$. Note that the objective value of (F-RH) is not necessarily an increasing function of σ for $\Sigma_N > 0$, because the rate of FOI can be negative if the information dissipated by the process noise dominates the information supplied by the measurement [12,13,15,16], in particular, when Σ_W is large.

When $M_V = I$ (i.e., $V_\tau = X_\tau$) and there is no process noise over $(\sigma, \tau]$, (F-RH) becomes equivalent to (S-RH), because then $\mathcal{I}(X_\sigma; \mathcal{Z}_{[0, \sigma]} | X_\tau) = 0$ as there is no remaining uncertainty in X_σ for a given X_τ . However, in general $\mathcal{I}(X_\sigma; \mathcal{Z}_{[0, \sigma]} | V_\tau) > 0$; therefore, the solutions to (S-RH) and (F-RH) differ. Also, the objective value of (F-RH) always overestimates that of (S-RH).

The difference between (S-RH) and (F-RH) can be explained in terms of information diffusion. It was shown in [17] that

$$\mathcal{I}(\mathcal{X}_{[\sigma, s]}; \mathcal{Z}_{[0, \sigma]}) = \mathcal{I}(X_\sigma; \mathcal{Z}_{[0, \sigma]}), \quad \forall s > \sigma \quad (11)$$

where $\mathcal{X}_{[t_1, t_2]} \triangleq \{X_s : s \in [t_1, t_2]\}$. This is because the sufficient statistics for estimation of the future state history $\mathcal{X}_{[\sigma, s]}$ is $\hat{X}_\sigma \triangleq \mathbb{E}[X_\sigma | \mathcal{Z}_{[0, \sigma]}]$, which is identical to that for estimating the current state X_σ based on the past measurement history $\mathcal{Z}_{[0, \sigma]}$.

The relation in (11) specifically holds for $s \geq \tau$. In this case, the verification variables at τ become a subset

of the future state history: i.e., $V_\tau \subset \mathcal{X}_{[\sigma, \tau]}$. Thus, what the filter-form on-the-fly information quantifies is the influence of the past measurement on the entire future, while the smoother-form on-the-fly information pinpoints the impact on some specified variables at some specific instant of time in the future. In this sense, the smoothing term in (S-RH), $\mathcal{I}(X_\sigma; \mathcal{Z}_{[0, \sigma]} | V_\tau)$ represents the portion of information gathered by $\mathcal{Z}_{[0, \sigma]}$ but will be diffused out to the space that is orthogonal to V_τ :

$$\mathcal{I}(X_\sigma; \mathcal{Z}_{[0, \sigma]} | V_\tau) = \mathcal{I}(\mathcal{X}_{[\sigma, \tau]} \setminus V_\tau; \mathcal{Z}_{[0, \sigma]} | V_\tau) \quad (12)$$

When $M_V = I$, (12) specifically means the information diffused through the future process noise: $\mathcal{I}(\mathcal{W}_{(\sigma, \tau]}; \mathcal{Z}_{[0, \sigma]} | X_\tau)$ where $\mathcal{W}_{(\sigma, \tau]} \triangleq \{W_s : s \in (\sigma, \tau]\}$. Note that $\mathcal{I}(\mathcal{W}_{(\sigma, \tau]}; \mathcal{Z}_{[0, \sigma]} | X_\tau)$ can be non-zero, although $\mathcal{I}(\mathcal{W}_{(\sigma, \tau]}; \mathcal{Z}_{[0, \sigma]}) = 0$ due to independence of $\mathcal{Z}_{[0, \sigma]}$ and $\mathcal{W}_{(\sigma, \tau]}$. These two become correlated to each other through the conditioning on X_τ , which is correlated to both of them.

The formulations (S-RH) and (F-RH) are written for the horizon starting from the initial time; extension to the decisions for a later horizon $[\sigma_k, \sigma_{k+1}]$ is straight-forward: they simply consider the conditioned mutual information conditioned on the previous measurement decision $\mathcal{Z}_{[0, \sigma_k]}^*$.

V. NUMERICAL EXAMPLES

This section presents numerical results to compare the two receding-horizon formulations discussed in section IV with three illustrative examples each of which reflects important aspects in the path planning problems.

A. Weather Forecasting

The first example is a simplified weather forecast problem introduced in [12]. An important aspect of this example is $M_V \neq I$. The state variables represent some scalar weather variable (e.g. temperature or pressure) at a total of n grid points. With the underlying nonlinear weather model – Lorenz-2003 chaos model with 72×17 grid space, a linear time-invariant model is obtained to represent short time-scale motion over some 4×3 local region, and process noise is introduced to represent the linearization error.

The goal of path planning is to reduce the entropy in the verification variables in 3 days (corresponding to some weather variables at some p grid points), by designing a 6-hr flight path for a single UAV sensor with constant speed v , whose motion is described by

$$\dot{x}_s = v \cos \theta, \quad \dot{y}_s = v \sin \theta, \quad \theta \in (-\pi, \pi]. \quad (13)$$

Although [12] originally posed this problem as a forecasting problem, this paper treats it as the decision for the first horizon of the tracking problem: namely, $\tau=3\text{days}$ and $\sigma=6\text{hrs}$.

Two scenarios with different configurations of local region, correlation length scale parameters, vehicle speed, and vehicle initial location, are considered. The performance of four different strategies are compared to each other: two are the receding-horizon formulations in (S-RH) and (F-RH). The other two strategies steer a sensor to climb up to the direction of the gradient of the information potential fields

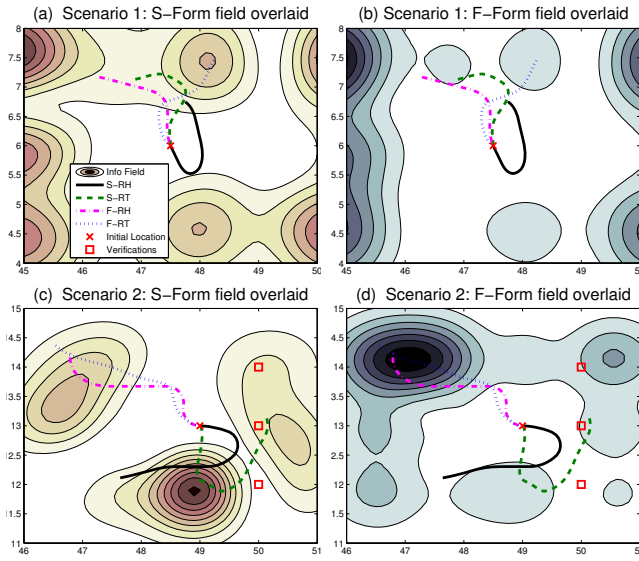


Fig. 1. Sensor trajectories for different strategies; x- and y-axis indicate the longitudinal and latitudinal grid indices; the smoother form and the filter form information fields are significantly different from each other for scenario 2.

TABLE I

INFORMATION GATHERED DURING THE FIRST HORIZON: $\mathcal{I}(V_\tau; \mathcal{Z}_{[0,\sigma]})$

Scenario	S-RH	S-RT	F-RH	F-RT
1	1.04	0.85	0.86	0.79
2	0.69	0.62	0.20	0.14

built on the basis of the rates of each on-the-fly information quantities (see [12,13] for details). These two strategies based on the information field are denoted as S-RT and F-RT.

Figs 1(a) and 1(b) illustrate the sensor trajectories from the four strategies for scenario 1 overlaid with the smoother-form and the filter-form information field at the initial time, respectively. In both information fields, a dark region represents an information-rich area. It can be seen that the shapes of the two information potential fields are similar in terms of the locations of information-rich regions; this leads to reasonable performance of filter-based planning (F-RH and F-RT) compared to smoother-based (S-RH and S-RT) (Table I). In contrast, Figures 1(c) and 1(d) illustrate the large difference between the information potential fields in scenario 2. As a consequence, the paths generated using S-RH and S-RT head southwards, while those from F-RH and F-RT head north, which leads to significant performance deterioration of the decisions based on the filter-form information (Table I).

In summary, this example demonstrates that a decision based on SOI and FOI can be very different depending on the problem. In this example, the process noise turns out not to be a dominant factor that causes the difference. The dominating factors are the fact that $\tau \gg \sigma$ and $M_V \neq I$.

B. Sensor Scheduling

A sensor scheduling problem with some artificial dynamics is considered as the second example; the key comparison made with this example is on the overall performance of

solutions from S-RH and F-RH. The system matrices are

$$A = \begin{bmatrix} 0.1 & -0.01 \\ 0.005 & 0.07 \end{bmatrix}, P_0 = \begin{bmatrix} 1 & -0.6 \\ -0.6 & 1 \end{bmatrix} \quad (14)$$

$$\Sigma_W = \text{diag}(0, 3), \Sigma_N = 1,$$

and $\tau = 5$. The planning horizon is 1, and for each planning cycle a decision is made either to measure the first state or the second one. Thus, the true optimal solution (OPT) can be found by simply enumerating all possible $32(=2^5)$ cases; S-RH and F-RH solutions can also be found by enumeration.

Fig. 2 illustrates the switching sequences for the three solutions. Observe that the three solutions are very different. In particular, the filter-form receding horizon solution is exactly opposite to the true optimal solution. Fig. 3 shows the information accumulation in the three solutions, where both the smoother-form accumulated information $\mathcal{I}(X_\tau; \mathcal{Z}_{[0,\sigma_k]})$ and the filter-form accumulated information $\mathcal{I}(X_{\sigma_k}; \mathcal{Z}_{[0,\sigma_k]})$ for $\sigma_k = 1, 2, \dots, 5$ are shown for comparison. Looking at the decisions for the first horizon: OPT and S-RF choose to measure state 1, but F-RH selects state 2. While the filter-form information indicates that measuring state 2 (follow dotted red line with marker \times) is slightly larger than that of measuring state 1 (follow dotted black line with marker \square), the smoother-form information indicates that the reward for observing state 1 is much larger than the other. It can be seen that the difference in this first decision leads to a larger gap in the final performance.

One important characteristic of the system in (14) is that a relatively large process noise is injected only to the dynamics of the second state variable. F-RH keeps measuring the second variable to compensate for the increase in the uncertainty in state 2 by the impact of the process noise over the time interval of size 1; however, in a long term view, the dynamics of the two variables are coupled and the effect of process noise is propagated to the first state variable. This results in a situation that F-RH is far from optimal. S-RH provides relatively good performance by taking account of the effect of the future process noise in the decision for each horizon.

C. Target Localization

The third example, which is adapted from [1], considers localization of a target whose location is fixed in a nominal sense using a mobile sensor. The main purpose of this example is to validate the presented receding-horizon formulation accounting for the nonlinearity in the measurement and replanning based on the actual measurement data.

The state vector X_t is defined to represent the position of the target, x_{tg} and y_{tg} . Since the target is assumed to be stationary, the system matrix $A = \mathbf{0}_{2 \times 2}$. The process noise represents the drift of the target position in the x - and y -directions;

$$\Sigma_W = \text{diag}(0.2^2, 0.01^2)$$

is used. Note that the target is subject to a larger drift in x -direction than y -direction. The sensor measures the bearing

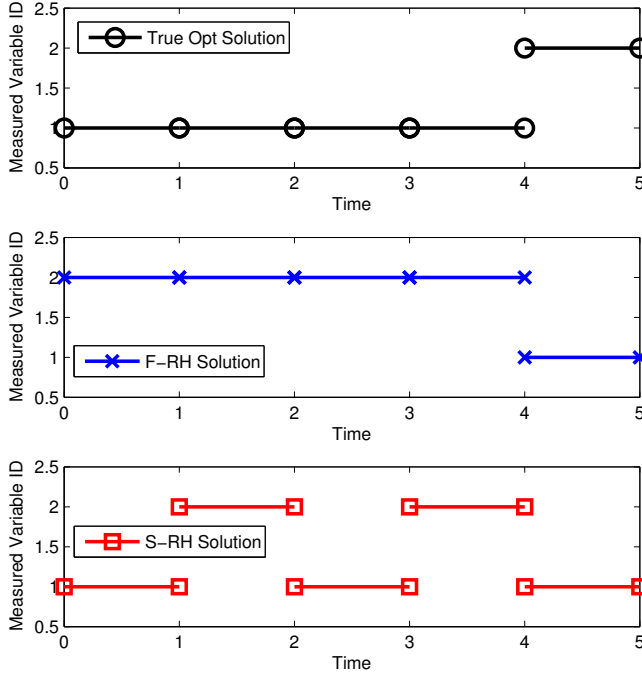


Fig. 2. Switching sequences for OPT, F-RH, and S-RH; F-RH solution behaves exactly opposite to OPT

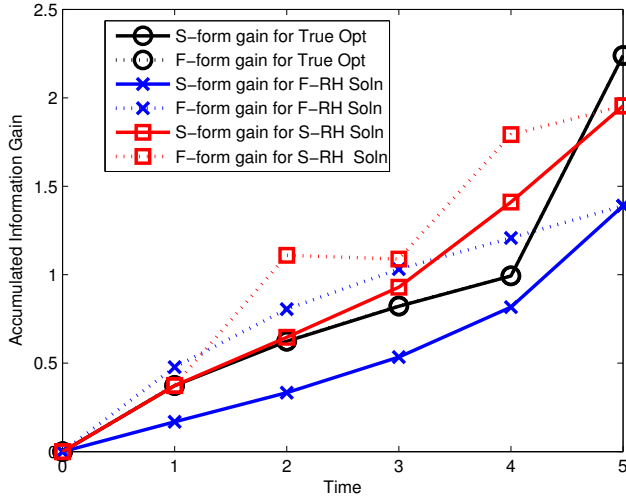


Fig. 3. Smoother-form and Filter-form information accumulation for OPT, F-RH, and S-RH; performance of F-RH is significantly worse than S-RH

angle between the target and itself:

$$Z_t = \tan^{-1}\{(y_{tg} - y_s)/(x_{tg} - x_s)\} + N_t \quad (15)$$

where the sensor's motion is described by (13). The target location is tracked by a *discrete* extended Kalman filter (EKF) using the bearing measurement taken with frequency of 16Hz with noise standard deviation of 2.5deg. Although the underlying estimator is discrete, the sensor planning problem for a horizon $[\sigma_k, \sigma_{k+1}]$ is posed in the continuous domain by linearizing (15) around the state estimate at σ_k . Then, the sensing noise intensity for this continuous planning becomes $\Sigma_N = 2.5^2(\pi/180)^2/16$. Once the plan for $[\sigma_k, \sigma_{k+1}]$ is made, the sensor executes it by moving along the planned path and taking discrete measurements every 1/16 seconds. The decision for the next horizon, $[\sigma_{k+1}, \sigma_{k+2}]$

is made by incorporating the actual measurement up to σ_{k+1} . The total length of the planning window is 14 seconds, which is divided into 14 receding planning horizons. Also, $P_0 = 0.5^2 I$ is used.

Fig. 4 shows the trajectories for S-RH and F-RH solutions with the true target locations over $[0, \tau]$, which are very different. The sensor moves mainly in y -direction in the S-RH solution but in x -direction in the F-RH solution. It can be seen in Fig. 5 that this difference in the path results in very different characteristics in reducing the uncertainty of the target location. The top two plots, which depict the time history of the entropy in the target's x - and y -positions, indicate that the S-RH solution mainly reduces the uncertainty in the estimate of y_{tg} , while F-RH reduces that of x_{tg} . In fact the entropy in x_{tg} increases along the S-RH path up to $t=8$ s. However, the bottom plot shows that the overall entropy does decrease over time. Since the target motion is mostly a drift in the x -direction, F-RH tries to reduce the uncertainty in x_{tg} due to the process noise. However, S-RH takes a different approach of reducing the uncertainty in y_{tg} and increasing the correlation between the estimates of x_{tg} and y_{tg} . The thinner lines in the bottom plot represent the summation of the entropy of x_{tg} and y_{tg} , so a large gap between this summation and the overall entropy (thicker lines) means high correlation between two position estimates. By looking at the overall entropy at $\tau=14$ s in the bottom plot of Fig. 5, it can be also seen that S-RH provides a slightly better performance than F-RH in this example. Since both S-RH and F-RH are suboptimal strategies and the (linear) model used for planning is updated using the actual (nonlinear) measurement in this example, consideration of the *modeled* future process noise in S-RH does not necessarily lead to significantly superior performance to F-RH. However, it is important to note the characteristics of the two receding-horizon formulations.

Fig. 6 illustrates the on-the-fly information (both S-Form and F-Form) used for the planning. The glitches seen every second are due to the modification of the linear model with the actual measurement values. Comparing the filter-form and the smoother-form information for the F-RH solution (blue solid and blue dash-dotted lines), it can be seen that the smoother-form information gathers a large amount of the information in the final phase (after 12s), while the filter-form assumes that it gathers almost a constant amount of information every time step after 2s. This information from the earlier time periods will experience the process noise for a longer time, and thus tends to be discounted in the smoother-form. Since in this example, the dynamics of x_{tg} and y_{tg} are decoupled from each other, this discounting effect is particularly prominent.

VI. CONCLUSIONS

This work discussed the roles of smoothing in solving the tracking class of informative path planning problems. It was demonstrated that the smoothing approach simplified the process of keeping track of information accumulation on the fly, by correctly calculating the information diffusion by

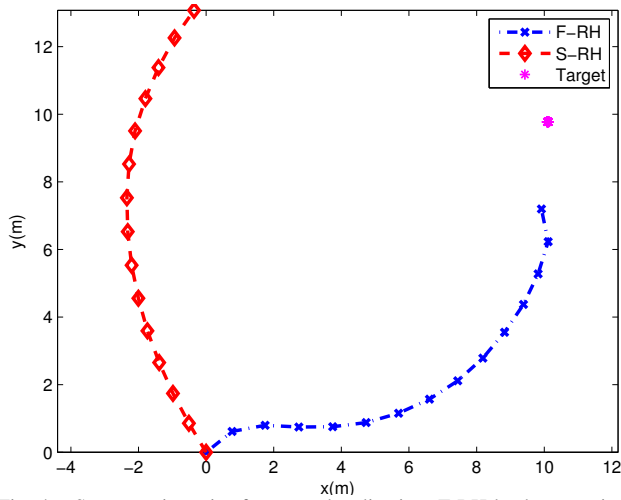


Fig. 4. Sensor trajectories for target localization: F-RH leads to motion in x -direction, while S-RH leads to motion in y -direction

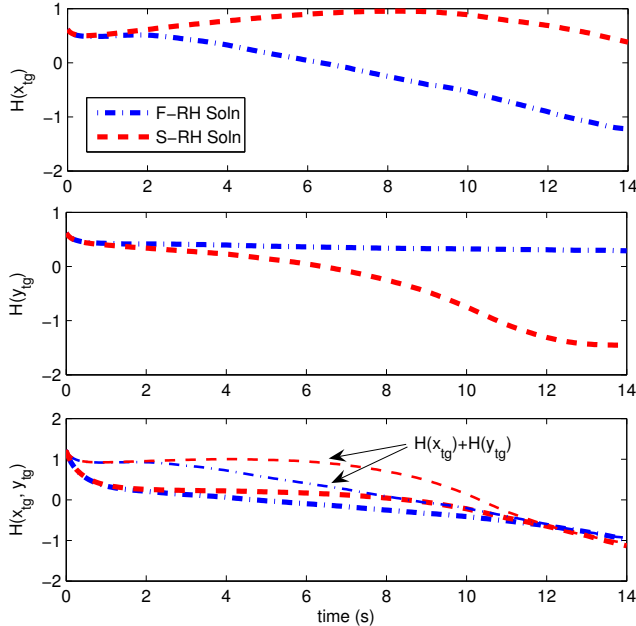


Fig. 5. Time histories of entropy of (a) target's x -position, (b) target's y -position, (c) overall position estimate: F-RH mainly reduces uncertainty in x -position while S-RH mainly reduces uncertainty in y -position

the future process noise. Numerical simulations with weather forecasting, sensor scheduling, and target localization examples indicated that smoothing offers significant advantages when the process noise is large, or when the verification variables are not the entire state.

ACKNOWLEDGMENT

This work is funded by NSF CNS-0540331 as part of the DDDAS program with Dr. Suhada Jayasuriya as the program manager.

REFERENCES

- [1] B. Grocholsky, "Information-theoretic control of multiple sensor platforms," Ph.D. dissertation, University of Sydney, 2002.
- [2] B. Grocholsky, A. Makarenko, and H. Durrant-Whyte, "Information-theoretic coordinated control of multiple sensor platforms," in *IEEE Intl. Conf. on Robotics and Automation*, Taipei, Taiwan, Sep. 2003, pp. 1521–1526.

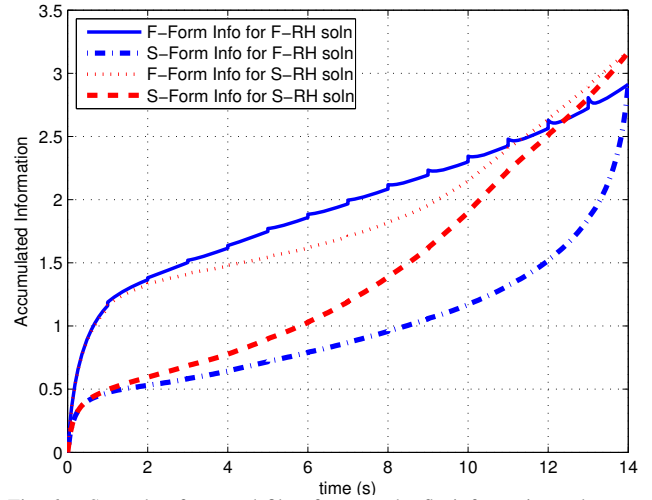


Fig. 6. Smoother-form and filter-form on-the-fly information values used for planning

- [3] B. Ristic and M. Arulampalam, "Tracking a manoeuvring target using angle-only measurements: algorithms and performance," *Signal Processing*, vol. 83, no. 6, pp. 1223–1238, 2003.
- [4] G. M. Hoffmann and C. Tomlin, "Mutual information methods with particle filters for mobile sensor network control," in *IEEE Conf. on Decision and Control*, 2006.
- [5] S. Martinez and F. Bullo, "Optimal Sensor Placement and Motion Coordination for Target Tracking," *Automatica*, vol. 42, pp. 661–668, 2006.
- [6] B. Grocholsky, J. Keller, V. Kumar, and J. Pappas, "Cooperative Air and Ground Surveillance," *IEEE Robotics and Automation Magazine*, vol. 13(3), pp. 16–25, 2006.
- [7] V. Gupta, T. H. Chung, B. Hassibi, and R. M. Murray, "On a stochastic sensor selection algorithm with applications in sensor scheduling and sensor coverage," *Automatica*, vol. 42(2), pp. 251–260, 2006.
- [8] J. L. Williams, J. W. Fisher III, and A. S. Willsky, "Approximate dynamic programming for communication-constrained sensor network management," *IEEE Trans. on Signal Processing*, vol. 55(8), pp. 3995–4003, 2007.
- [9] S. Majumdar, C. Bishop, B. Etherton, and Z. Toth, "Adaptive sampling with the ensemble transform Kalman filter. Part II: Field programming implementation," *Monthly Weather Review*, vol. 130, no. 3, pp. 1356–1369, 2002.
- [10] H.-L. Choi, J. P. How, and J. A. Hansen, "Ensemble-based adaptive targeting of mobile sensor networks," in *American Control Conference*, 2007.
- [11] H.-L. Choi and J. P. How, "A multi-UAV targeting algorithm for ensemble forecast improvement," in *AIAA Guidance, Navigation, and Control Conference*, 2007.
- [12] —, "Continuous motion planning for information forecast," in *IEEE Conf. on Decision and Control*, Cancun, Mexico, Dec. 2008, pp. 1721–1728.
- [13] —, "Continuous trajectory planning of mobile sensors for informative forecasting," *Automatica*, submitted.
- [14] F. Hover, "Continuous-time adaptive sampling and forecast assimilation for autonomous vehicles," Presentation given to WHOI Department of Applied Ocean Physics and Engineering, <http://web.mit.edu/hovergroup/pub/PPIDA.pdf>, Oct. 2008.
- [15] E. Mayer-Wolf and M. Zakai, "On a formula relating the Shannon information to the Fisher information for the filtering problem," *Lecture Notes in Control and Information Sciences* 61, pp. 164–171, 1984.
- [16] S. Mitter and N. Newton, "Information and entropy flow in the Kalman-Bucy filter," *Journal of Statistical Physics*, vol. 118, no. 112, pp. 145–176, 2005.
- [17] N. Newton, "Dual nonlinear filters and entropy production," *SIAM Journal on Control and Optimization*, vol. 45, no. 3, pp. 998–1016, 2006.